

Fast and Efficient Preparation of Exfoliated 2H MoS₂ Nanosheets by Sonication-Assisted Lithium Intercalation and Infrared Laser-Induced 1T to 2H Phase Reversion

Xiaobin Fan,^{†,‡} Pengtao Xu,[†] Dekai Zhou,[†] Yifan Sun,[†] Yuguang C. Li,[†] Minh An T. Nguyen,[†] Mauricio Terrones,[†] and Thomas E. Mallouk^{*,†}

[†]Departments of Chemistry, Biochemistry and Molecular Biology, and Physics, The Pennsylvania State University, University Park, Pennsylvania 16802, United States

[‡]State Key Laboratory of Chemical Engineering, Collaborative Innovation Center of Chemical Science and Engineering, School of Chemical Engineering and Technology, Tianjin University, Tianjin 300072, China

Supporting Information

ABSTRACT: Exfoliated 2H molybdenum disulfide (MoS₂) has unique properties and potential applications in a wide range of fields, but corresponding studies have been hampered by the lack of effective routes to it in bulk quantities. This study presents a rapid and efficient route to obtain exfoliated 2H MoS₂, which combines fast sonication-assisted lithium intercalation and infrared (IR) laser-induced phase reversion. We found that the complete lithium intercalation of MoS₂ with butyllithium could be effected within 1.5 h with the aid of sonication. The 2H to 1T phase transition that occurs during the lithium intercalation could be also reversed by IR laser irradiation with a DVD optical drive.

KEYWORDS: MoS₂, exfoliation, intercalation, sonication, infrared laser



Two-dimensionally bonded transition-metal dichalcogenides (TMDs),^{1–4} especially monolayer molybdenum disulfide (MoS₂), possess unique physical and chemical properties and potential utility as hydrogen evolution catalysts^{5–8} and components of electronic and optoelectronic devices.^{9–22} However, fundamental studies and practical applications of MoS₂ (and related TMDs) have been hampered by the lack of effective routes to bulk quantities of undamaged single-layer, semiconducting nanosheets. MoS₂ exhibits a layered structure with strong covalent Mo–S bonds in plane and van der Waals bonding between sheets.²³ This weak interlayer bonding enables “top-down” mechanical or chemical exfoliation. Unlike bottom-up strategies such as chemical vapor deposition,^{24–28} top-down approaches can start from abundant natural crystals or intentionally doped synthetic crystals to produce macroscopic quantities of exfoliated MoS₂. However, the production of monolayer MoS₂ nanosheets by mechanical exfoliation methods has so far been challenging because of the low yield of monolayer products in microexfoliation,²⁹ sonication-assisted liquid-exfoliation,^{30–32} and shear exfoliation.^{33,34} The chemical route,^{35–43} normally involving non-aqueous lithium intercalation followed by a water exfoliation step, requires a lengthy (24 h or days) intercalation step,^{35–37} sophisticated electrochemical control^{38–40} or additional pre-expanding treatment.⁴¹ While it is effective in expanding the layers, the exothermic reaction of water with Li_xMoS₂ produces a corrosive alkaline medium, which over long reaction times can substantially damage the sheets. In addition, the lithium intercalation reaction transforms MoS₂ from the hexagonal

structure (2H phase) it has in its pristine form to the trigonal 1T phase.^{35–42} This change from trigonal prismatic to octahedral coordination of Mo compromises the semiconducting properties of the sheets.

In this study, we report a rapid and efficient route to exfoliated 2H MoS₂, which combines fast sonication-assisted lithium intercalation and infrared laser-induced phase reversion as illustrated in Scheme 1. The exfoliation process explored in this paper combined the reaction of *n*-butyllithium (BuLi), a convenient reagent for the complete intercalation of MoS₂ to stoichiometric LiMoS₂,³⁵ with sonication. We found that lithium intercalation in BuLi/hexane solution could be significantly accelerated by sonication and that complete intercalation occurred within minutes under mild sonication conditions (135 W, ~1.5 h).

The progress of the reaction was monitored by X-ray diffraction (XRD). XRD patterns of freshly intercalated samples periodically taken from the reaction mixture are shown in Figure 1. The characteristic peaks of hexagonal 2H MoS₂ (blue) quickly disappear within 60 min during the intercalation reaction, and new peaks corresponding to the intercalated phase emerge at the same time. It is well-known that ultrasound can accelerate reactions by acoustic cavitation, which produces intense local heating and high pressures. These effects should increase the rate of reaction between BuLi and MoS₂.

Received: May 28, 2015

Revised: August 5, 2015

Published: August 19, 2015

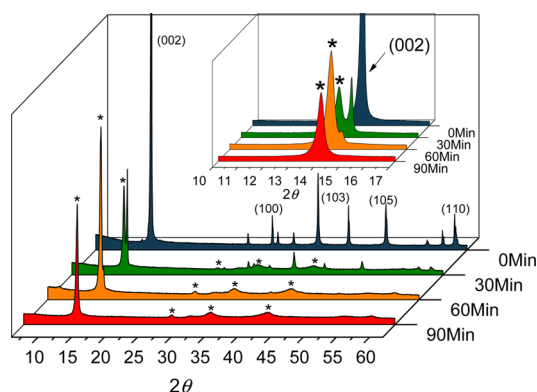
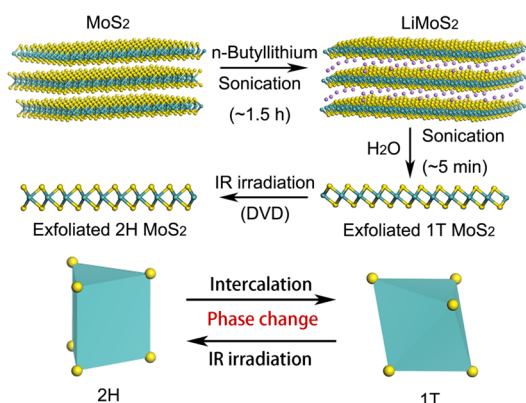
Scheme 1. Reaction Scheme for the Preparation of Exfoliated 2H MoS₂


Figure 1. Progression of XRD patterns obtained during the sonication-assisted lithium intercalation of MoS₂. Note that only the main peaks were noted according to JCPDS 37-1492, and the reflections of the intercalated compounds are marked by black asterisks. The inset shows the evolution of the MoS₂ (002) reflection during the intercalation reaction, where the (001) reflections of the intercalated compounds are marked by black asterisks.

Sonication is also known to facilitate the transient expansion and exfoliation of layered materials in liquid suspensions, which can help overcome the activation barrier for intercalation.⁴⁴ Close examination of the (002) peak confirms the rapid decay of its intensity and the rise of a new adjacent peak at lower angle, attributed to the *c*-axis expansion of the intercalated compound. The spacing between the adjacent layers of the intercalated phase is ~ 6.31 Å, which is ~ 0.15 Å larger than that of the pristine MoS₂ and matches the theoretical interlayer spacing of LiMoS₂. Note that aging the LiMoS₂ samples in air results in a further shift of its (001) reflection toward lower angle and the hydration of the intercalated Li ions (Figure S2, Supporting Information). X-ray photoelectron spectroscopy (XPS) shows that both the Mo 3d_{5/2} and Mo 3d_{3/2} peaks gradually split into two independent regions (Figure S12, Supporting Information), attributed to the well-known 2H–1T phase transition during the intercalation reaction. In line with previous studies,³⁷ the completely intercalated samples are predominantly the 1T phase. This phase transition is driven by electron transfer from Li to MoS₂, which destabilizes the trigonal prismatic coordination of Mo beyond a *d*-electron count of two per atom.³

Typical scanning electron microscope (SEM) images of the intercalated samples show heavy cracking of their surfaces and

edges (Figure S4, Supporting Information), suggesting their ready exfoliation in water. In fact, fresh, completely intercalated samples can react with water and form exfoliated monolayer MoS₂ nanosheets when they are sonicated in water for only ~ 5 min, and incompletely intercalated samples can be exfoliated over longer periods of time (Figure S9 and S10, Supporting Information). However, complete exfoliation of aged samples into single-layer nanosheets does not occur even after sonication in water for 1 h (Figure S5, Supporting Information), despite the increased interlayer distance in Li_{*x*}(H₂O)_{*y*}MoS₂. Based on these observations, the surface cracking and reactivity of intercalated samples induced by sonication appears to play a key role in the efficiency of exfoliation. The highest yield of single-layer products is found when the solid is exfoliated immediately after intercalation.

Transmission electron microscopy (TEM) images of exfoliated MoS₂ shows translucent nanosheets (Figure 2a)

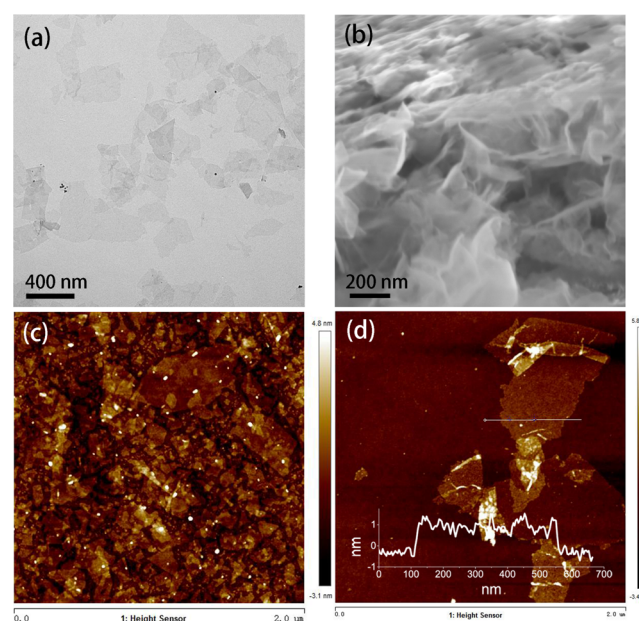


Figure 2. Representative TEM, SEM, and AFM images of exfoliated MoS₂. The scale bars in a and b are 400 and 200 nm, respectively. The scan sizes of AFM images in c and d are 2 μ m.

with obvious wrinkles and folds as revealed by SEM (Figure 2b). Prolonged sonication of the completely intercalated products in water leads to a dramatic decrease in the lateral size of the sheets (Figure S9 and S11, Supporting Information), attributed to the corrosion of single-layer MoS₂ in the alkaline medium. The monolayer nature of the exfoliated sheets was confirmed by atomic force microscopy (AFM). Based on the AFM analysis of the exfoliated products prior to purification (Figure 2c), the yield of single sheets can be roughly estimated at $>95\%$, and the exfoliated sheets have a dominant lateral size of about 300 nm. Folded exfoliated sheets with lateral size over 2 μ m can be occasionally found (Figure S7, Supporting Information). Normally, individual sheets measured by AFM (Figure 2d) have an average thickness of ~ 1.2 nm, in line with the reported apparent thickness of a chemically exfoliated monolayer of MoS₂. Note that this value is somewhat larger than the theoretical thickness of monolayer MoS₂ and flat samples prepared by mechanical exfoliation methods, and it is

attributed to an intrinsic out-of-plane deformation of 0.6–1 nm.^{45,46}

Despite its efficiency in producing monolayer MoS₂, the chemical intercalation/exfoliation route always results in the loss of the semiconducting properties of pristine MoS₂, because of the 2H to 1T phase change during Li intercalation.⁴² In order to reverse this transformation, exfoliated MoS₂ sheets are typically annealed or heated in high boiling organic solvents at temperatures of 100–300 °C under an inert atmosphere.^{37,47} Considering the metastable nature of the metallic 1T phase of MoS₂ and the intrinsic strong infrared (IR) absorption of metallic materials (such as the 1T MoS₂), we hypothesized that the 1T phase could be thermally converted back to the 2H phase when exposed to IR radiation. This hypothesis was confirmed as shown in Figure 3a. A thin film of chemically

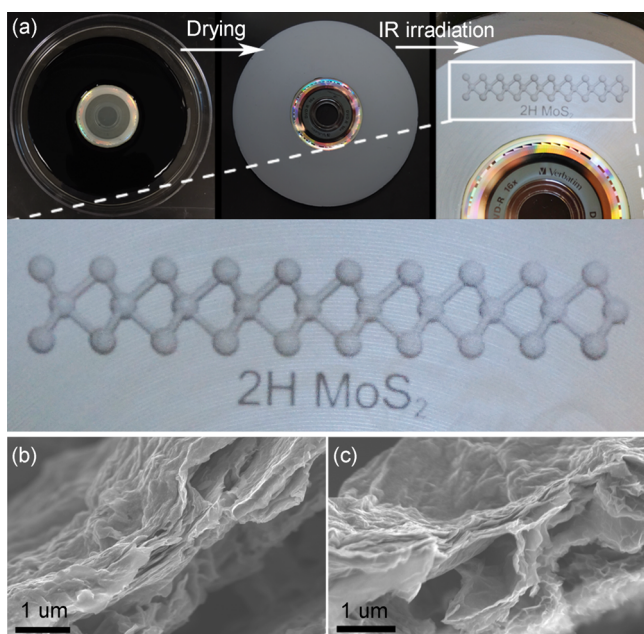


Figure 3. (a) IR laser-induced transformation of restacked 1T MoS₂ nanosheets to 2H MoS₂; the image written on the DVD is a ball-and-stick drawing of a 2H MoS₂ layer. Typical SEM images of exfoliated MoS₂ before (b) and after IR irradiation (c).

exfoliated MoS₂ dispersed in water was drop-cast onto DVD discs and irradiated with the near-IR laser of a commercial DVD optical drive. The 1T–2H phase transformation is indicated by the change in color from dark to light gray. Using the write capability of the LightScribe DVD drive, this transformation could be done in any designed pattern as illustrated. In keeping with the TEM, SEM, and AFM results above, cross-sectional SEM images of the deposited films show well-exfoliated wrinkled sheets (Figure 3b) and no noticeable changes in morphology after conversion to the 2H phase by irradiation (Figure 3c).

Raman spectroscopic analysis confirms the successful 1T–2H phase transition of exfoliated MoS₂. Consistent with previous studies of the 1T phase,^{37,48} chemically exfoliated MoS₂ before irradiation (Figure 4a) shows additional J₁, J₂, and J₃ peaks that are attributed to the superlattice structure of 1T MoS₂ nanosheets. The presence of the E_{1g} band at 284–307 cm⁻¹ along with the weak E_{2g} band confirms the dominant octahedral coordination of Mo in 1T MoS₂. After irradiation with IR (Figure 4b), the Raman signals of the characteristic in-

plane E_{2g}¹ and out-of-plane A_{1g} modes of MoS₂ substantially increase, in concert with the disappearance of the J₁, J₂, J₃, and E_{1g} peaks. These distinct changes confirm the 1T–2H phase reversion and are supported by further analysis by XPS.³⁷ Like the intercalated products before exfoliation, chemically exfoliated MoS₂ nanosheets consist predominantly of the 1T phase before IR irradiation (Figure 4c). The 1T peaks disappear completely upon IR irradiation (Figure 4d). It should be noted that the Mo⁶⁺ peak increases slightly during irradiation, most likely because of partial air oxidation of the MoS₂ surface.

The metallic to semiconducting transition was confirmed by the diffuse reflectance UV–vis–NIR spectroscopy. As shown in Figure 4e, the deposited exfoliated MoS₂ film before irradiation has a featureless spectrum with a strong absorption band in the near-IR region and the expected stronger absorption in the mid and far-IR regions, attributed to the metallic 1T phase. The characteristic direct-gap transitions (transitions A and B)³⁹ between the lowest conduction band and the highest valence split bands at the K-point of 2H MoS₂ emerge after irradiation, due to the 1T–2H phase reversion. A plot of the transformed Kubelka–Munk function versus photon energy reveals that the direct band gap of irradiated MoS₂ is ~1.71 eV (Figure 4f). This value is larger than the indirect band gap of bulk MoS₂ (~1.3 eV) and matches the band gap of monolayer 2H MoS₂ (~1.8 eV).⁴⁹ Taken together, these results demonstrate the successful 1T–2H phase reversion and the restoration of semiconducting properties from the chemically exfoliated MoS₂.

In summary, we have developed a rapid and efficient method for preparing exfoliated 2H MoS₂ from bulk crystals. The complete lithium intercalation of MoS₂ with BuLi could be effected within 1.5 h with the aid of sonication, which is significantly faster than has been reported by conventional methods. The 2H to 1T phase transition that occurs during the intercalation process can be reversed by IR laser irradiation, restoring the semiconducting properties of the nanosheets. In films with thicknesses of a few microns, exfoliated 1T MoS₂ can be readily converted to its 2H counterpart by using a DVD optical drive as the light source. The methods described here should be easily adaptable to the preparation of doped MoS₂ and other exfoliated TMDs from the appropriate parent crystals on a bulk scale.

Methods. Intercalation and Exfoliation of MoS₂. Typically, the intercalation of MoS₂ was carried out by sonicating (135 W, Branson 5510) 2 g MoS₂ crystals (Acros Organics) with BuLi/hexane solution (10 mL, 5 M, Sigma-Aldrich) in a 50 mL Schlenk flask for ~1.5 h. This procedure could be scaled up, and optimization of the intercalation process could be achieved by adjusting the water level of the sonication bath. Excess BuLi was recovered by filtration or by dilution with hexane, and the intercalated samples were retrieved by centrifugation and washed three times with 40 mL of hexane to remove excess lithium and organic residues. Standard air-free techniques were employed by using a Schlenk line or a glovebox under the protection of inert gas. Exfoliation was achieved by immediately sonicating the freshly intercalated samples in water for about 5 min, and the exfoliated samples were purified by centrifugation.

IR Laser-Induced 1T–2H Phase Transition. Exfoliated MoS₂ thin films on the DVD discs were prepared by drop-casting ~15 mL of the exfoliated MoS₂ dispersion onto the top-side of DVD discs (Verbatim) and drying for >24 h at ambient temperature. The films were irradiated in air with the near-IR laser inside the

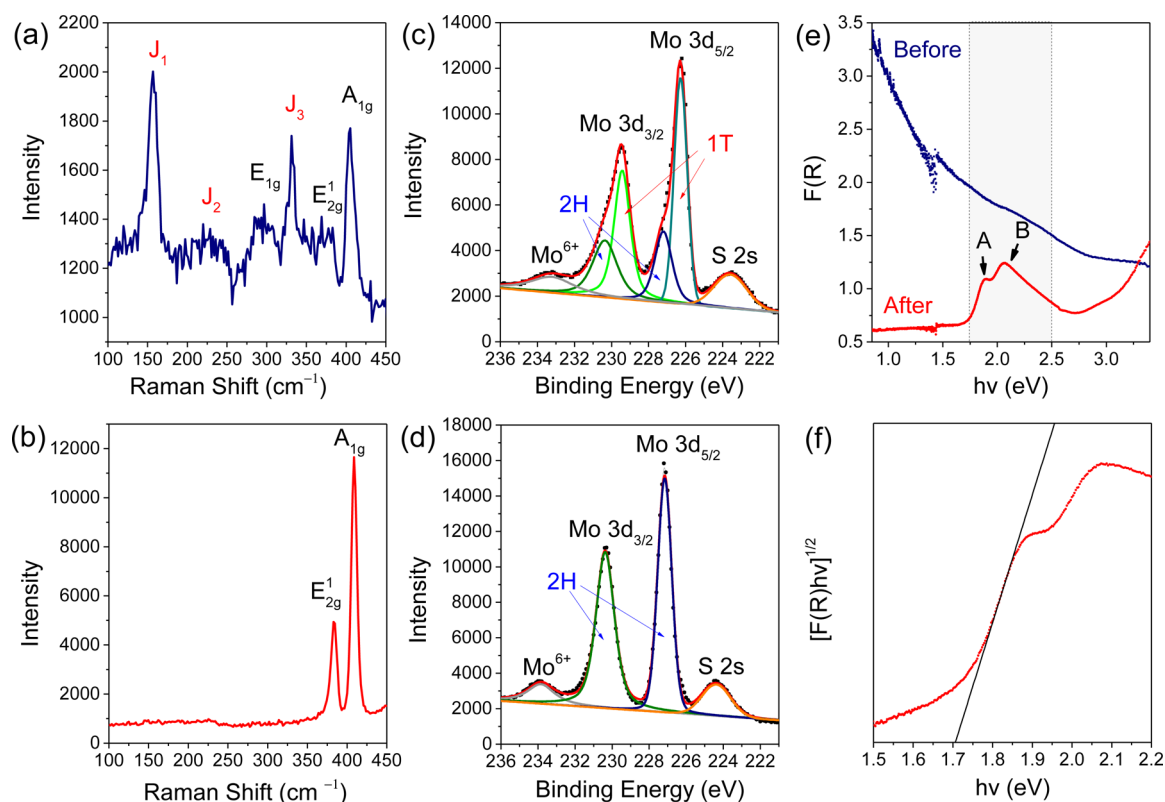


Figure 4. Raman spectra of the chemically exfoliated MoS₂ before (a) and after irradiation (b). Note that different Raman intensities were observed under the same characterization conditions with 514.5 nm laser excitation, and the Raman peak positions of the obtained exfoliated 2H MoS₂ are not sensitive to the layer number in the restacked films;³⁷ Mo 3d and S 2s XPS spectra of chemically exfoliated MoS₂ before (c) and after (d) IR irradiation. The 2H and 1T phases show a difference in binding energy of about 0.9 eV; (e) diffuse reflectance UV-vis-NIR spectra of the deposited MoS₂ film before (blue line) and after irradiation (red line); (f) plot of the transformed Kubelka-Munk function vs photon energy for the irradiated MoS₂ film. The energy value at the point of intersection of the tangent line and the horizontal axis is the optical band gap.

commercial LightScribe DVD optical drive⁵⁰ (LG GE20LU10, 40 mW as objective emission light of 780 nm wavelength). For films with thicknesses of few microns, the 1T–2H phase reversion was complete after one write cycle, consistent with the relatively long penetration depth of near-IR radiation.

Characterization. Samples were characterized by XRD (Philips Empyrean, Cu-K α radiation), TEM (JEOL 1200 EXII), AFM (Bruker Icon microscope, peak force tapping mode), SEM (FEI NanoSEM 630 FESEM), Raman (Renishaw inVia confocal microscope-based Raman spectrometer with 514.5 nm laser excitation), X-ray photoelectron spectroscopy (Kratos Analytical Axis Ultra), and a UV-vis-NIR spectrophotometer (PerkinElmer Lambda 950).

■ ASSOCIATED CONTENT

Supporting Information

The Supporting Information is available free of charge on the ACS Publications website at DOI: 10.1021/acs.nanolett.5b02091.

XRD patterns from control experiments and the intercalated samples after exposure to air for different periods of time; SEM images of the intercalated compounds; AFM images of exfoliated samples; XPS spectra of the intercalated and exfoliated samples; Raman spectra of films after IR irradiation; SEM images and optical images of deposited films (PDF)

■ AUTHOR INFORMATION

Corresponding Author

*E-mail: tem5@psu.edu.

Notes

The authors declare no competing financial interest.

■ ACKNOWLEDGMENTS

This work is supported by the U.S. Army Research Office MURI grant W911NF-11-1-0362. The authors also acknowledge the Natural Science Funds for Excellent Young Scholars (No. 21222608) and the Program of Introducing Talents of Discipline to Universities (No. B06006).

■ REFERENCES

- (1) Xu, M. S.; Liang, T.; Shi, M. M.; Chen, H. Z. *Chem. Rev.* **2013**, *113*, 3766–3798.
- (2) Huang, X.; Zeng, Z. Y.; Zhang, H. *Chem. Soc. Rev.* **2013**, *42*, 1934–1946.
- (3) Chhowalla, M.; Shin, H. S.; Eda, G.; Li, L. J.; Loh, K. P.; Zhang, H. *Nat. Chem.* **2013**, *5*, 263–275.
- (4) Najmaei, S.; Yuan, J. T.; Zhang, J.; Ajayan, P.; Lou, J. *Acc. Chem. Res.* **2015**, *48*, 31–40.
- (5) Jaramillo, T. F.; Jorgensen, K. P.; Bonde, J.; Nielsen, J. H.; Horch, S.; Chorkendorff, I. *Science* **2007**, *317*, 100–102.
- (6) Kibsgaard, J.; Chen, Z. B.; Reinecke, B. N.; Jaramillo, T. F. *Nat. Mater.* **2012**, *11*, 963–969.
- (7) Travert, A.; Nakamura, H.; van Santen, R. A.; Cristol, S.; Paul, J. F.; Payen, E. *J. Am. Chem. Soc.* **2002**, *124*, 7084–7095.

- (8) Voiry, D.; Salehi, M.; Silva, R.; Fujita, T.; Chen, M. W.; Asefa, T.; Shenoy, V. B.; Eda, G.; Chhowalla, M. *Nano Lett.* **2013**, *13*, 6222–6227.
- (9) Lembke, D.; Bertolazzi, S.; Kis, A. *Acc. Chem. Res.* **2015**, *48*, 100–110.
- (10) Yoon, Y.; Ganapathi, K.; Salahuddin, S. *Nano Lett.* **2011**, *11*, 3768–3773.
- (11) Wang, Q. H.; Kalantar-Zadeh, K.; Kis, A.; Coleman, J. N.; Strano, M. S. *Nat. Nanotechnol.* **2012**, *7*, 699–712.
- (12) Li, X. F.; Yang, L. M.; Si, M. W.; Li, S. C.; Huang, M. Q.; Ye, P. D.; Wu, Y. Q. *Adv. Mater.* **2015**, *27*, 1547–1552.
- (13) Butun, S.; Tongay, S.; Aydin, K. *Nano Lett.* **2015**, *15*, 2700–2704.
- (14) Kwon, J.; Hong, Y. K.; Han, G.; Omkaram, I.; Choi, W.; Kim, S.; Yoon, Y. *Adv. Mater.* **2015**, *27*, 2224–2230.
- (15) Jariwala, D.; Sangwan, V. K.; Lauhon, L. J.; Marks, T. J.; Hersam, M. C. *ACS Nano* **2014**, *8*, 1102–1120.
- (16) Yin, Z. Y.; Li, H.; Li, H.; Jiang, L.; Shi, Y. M.; Sun, Y. H.; Lu, G.; Zhang, Q.; Chen, X. D.; Zhang, H. *ACS Nano* **2012**, *6*, 74–80.
- (17) Xiao, J.; Choi, D. W.; Cosimbescu, L.; Koeh, P.; Liu, J.; Lemmon, J. P. *Chem. Mater.* **2010**, *22*, 4522–4524.
- (18) Wang, J. A.; Feng, B.; Wu, W. G.; Huang, Y. *Microelectron. Eng.* **2011**, *88*, 1019–1023.
- (19) Zhu, C. F.; Zeng, Z. Y.; Li, H.; Li, F.; Fan, C. H.; Zhang, H. J. *Am. Chem. Soc.* **2013**, *135*, 5998–6001.
- (20) Choi, M. S.; Lee, G. H.; Yu, Y. J.; Lee, D. Y.; Lee, S. H.; Kim, P.; Hone, J.; Yoo, W. J. *Nat. Commun.* **2013**, *4*, 1624.
- (21) Tang, H. J.; Wang, J. Y.; Yin, H. J.; Zhao, H. J.; Wang, D.; Tang, Z. Y. *Adv. Mater.* **2015**, *27*, 1117–1123.
- (22) Mukherjee, S.; Maiti, R.; Midya, A.; Das, S.; Ray, S. K. *ACS Photonics* **2015**, *2*, 760.
- (23) Lv, R.; Robinson, J. A.; Schaak, R. E.; Sun, D.; Sun, Y. F.; Mallouk, T. E.; Terrones, M. *Acc. Chem. Res.* **2015**, *48*, 56–64.
- (24) van der Zande, A. M.; Huang, P. Y.; Chenet, D. A.; Berkelbach, T. C.; You, Y. M.; Lee, G. H.; Heinz, T. F.; Reichman, D. R.; Muller, D. A.; Hone, J. C. *Nat. Mater.* **2013**, *12*, 554–561.
- (25) Lee, Y. H.; Zhang, X. Q.; Zhang, W. J.; Chang, M. T.; Lin, C. T.; Chang, K. D.; Yu, Y. C.; Wang, J. T. W.; Chang, C. S.; Li, L. J.; Lin, T. W. *Adv. Mater.* **2012**, *24*, 2320–2325.
- (26) Najmaei, S.; Liu, Z.; Zhou, W.; Zou, X. L.; Shi, G.; Lei, S. D.; Yakobson, B. I.; Idrobo, J. C.; Ajayan, P. M.; Lou, J. *Nat. Mater.* **2013**, *12*, 754–759.
- (27) Ling, X.; Lee, Y. H.; Lin, Y. X.; Fang, W. J.; Yu, L. L.; Dresselhaus, M. S.; Kong, J. *Nano Lett.* **2014**, *14*, 464–472.
- (28) Han, G. H.; Kybert, N. J.; Naylor, C. H.; Lee, B. S.; Ping, J. L.; Park, J. H.; Kang, J.; Lee, S. Y.; Lee, Y. H.; Agarwal, R.; Johnson, A. T. C. *Nat. Commun.* **2015**, *6*, 6128.
- (29) Novoselov, K. S.; Jiang, D.; Schedin, F.; Booth, T. J.; Khotkevich, V. V.; Morozov, S. V.; Geim, A. K. *Proc. Natl. Acad. Sci. U. S. A.* **2005**, *102*, 10451–10453.
- (30) Coleman, J. N.; Lotya, M.; O'Neill, A.; Bergin, S. D.; King, P. J.; Khan, U.; Young, K.; Gaucher, A.; De, S.; Smith, R. J.; Shvets, I. V.; Arora, S. K.; Stanton, G.; Kim, H. Y.; Lee, K.; Kim, G. T.; Duesberg, G. S.; Hallam, T.; Boland, J. J.; Wang, J. J.; Donegan, J. F.; Grunlan, J. C.; Moriarty, G.; Shmeliov, A.; Nicholls, R. J.; Perkins, J. M.; Grievson, E. M.; Theuwissen, K.; McComb, D. W.; Nellist, P. D.; Nicolosi, V. *Science* **2011**, *331*, 568–571.
- (31) Yu, X. Y.; Prevot, M. S.; Sivula, K. *Chem. Mater.* **2014**, *26*, 5892–5899.
- (32) Guan, G. J.; Zhang, S. Y.; Liu, S. H.; Cai, Y. Q.; Low, M.; Teng, C. P.; Phang, I. Y.; Cheng, Y.; Duei, K. L.; Srinivasan, B. M.; Zheng, U. G.; Zhang, Y. W.; Han, M. Y. *J. Am. Chem. Soc.* **2015**, *137*, 6152–6155.
- (33) Paton, K. R.; Varrla, E.; Backes, C.; Smith, R. J.; Khan, U.; O'Neill, A.; Boland, C.; Lotya, M.; Istrate, O. M.; King, P.; Higgins, T.; Barwich, S.; May, P.; Puczkarski, P.; Ahmed, I.; Moebius, M.; Pettersson, H.; Long, E.; Coelho, J.; O'Brien, S. E.; McGuire, E. K.; Sanchez, B. M.; Duesberg, G. S.; McEvoy, N.; Pennycook, T. J.; Downing, C.; Crossley, A.; Nicolosi, V.; Coleman, J. N. *Nat. Mater.* **2014**, *13*, 624–630.
- (34) Varrla, E.; Backes, C.; Paton, K. R.; Harvey, A.; Gholamvand, Z.; McCauley, J.; Coleman, J. N. *Chem. Mater.* **2015**, *27*, 1129–1139.
- (35) Joensen, P.; Frindt, R. F.; Morrison, S. R. *Mater. Res. Bull.* **1986**, *21*, 457–461.
- (36) Knirsch, K. C.; Berner, N. C.; Nerl, H. C.; Cucinotta, G. S.; Gholamvand, Z.; McEvoy, N.; Wang, Z. X.; Abramovic, I.; Vecera, P.; Halik, M.; Sanvito, S.; Duesberg, G. S.; Nicolosi, V.; Hauke, F.; Hirsch, A.; Coleman, J. N.; Backes, C. *ACS Nano* **2015**, *9*, 6018.
- (37) Eda, G.; Yamaguchi, H.; Voiry, D.; Fujita, T.; Chen, M. W.; Chhowalla, M. *Nano Lett.* **2011**, *11*, 5111–5116.
- (38) Zeng, Z. Y.; Yin, Z. Y.; Huang, X.; Li, H.; He, Q. Y.; Lu, G.; Boey, F.; Zhang, H. *Angew. Chem., Int. Ed.* **2011**, *50*, 11093–11097.
- (39) Eng, A. Y. S.; Ambrosi, A.; Sofer, Z.; Simek, P.; Pumera, M. *ACS Nano* **2014**, *8*, 12185–12198.
- (40) Liu, N.; Kim, P.; Kim, J. H.; Ye, J. H.; Kim, S.; Lee, C. J. *ACS Nano* **2014**, *8*, 6902–6910.
- (41) Zheng, J.; Zhang, H.; Dong, S. H.; Liu, Y. P.; Nai, C. T.; Shin, H. S.; Jeong, H. Y.; Liu, B.; Loh, K. P. *Nat. Commun.* **2014**, *5*, 2995.
- (42) Cheng, Y. C.; Nie, A. M.; Zhang, Q. Y.; Gan, L. Y.; Shahbazian-Yassar, R.; Schwingenschlogl, U. *ACS Nano* **2014**, *8*, 11447–11453.
- (43) Gordon, R. A.; Yang, D.; Crozier, E. D.; Jiang, D. T.; Frindt, R. F. *Phys. Rev. B: Condens. Matter Mater. Phys.* **2002**, *65*, 125407.
- (44) Nicolosi, V.; Chhowalla, M.; Kanatzidis, M. G.; Strano, M. S.; Coleman, J. N. *Science* **2013**, *340*, 1420.
- (45) Brivio, J.; Alexander, D. T. L.; Kis, A. *Nano Lett.* **2011**, *11*, 5148–5153.
- (46) Luo, S. W.; Hao, G. L.; Fan, Y. P.; Kou, L. Z.; He, C. Y.; Qi, X.; Tang, C.; Li, J.; Huang, K.; Zhong, J. X. *Nanotechnology* **2015**, *26*, 105705.
- (47) Chou, S. S.; Huang, Y. K.; Kim, J.; Kaehr, B.; Foley, B. M.; Lu, P.; Dykstra, C.; Hopkins, P. E.; Brinker, C. J.; Huang, J. X.; Draid, V. P. *J. Am. Chem. Soc.* **2015**, *137*, 1742–1745.
- (48) Sandoval, S. J.; Yang, D.; Frindt, R. F.; Irwin, J. C. *Phys. Rev. B: Condens. Matter Mater. Phys.* **1991**, *44*, 3955–3962.
- (49) Splendiani, A.; Sun, L.; Zhang, Y. B.; Li, T. S.; Kim, J.; Chim, C. Y.; Galli, G.; Wang, F. *Nano Lett.* **2010**, *10*, 1271–1275.
- (50) El-Kady, M. F.; Strong, V.; Dubin, S.; Kaner, R. B. *Science* **2012**, *335*, 1326–1330.